Article

Experimental Analysis of a Vertical Drop Shaft

Roberta Padulano *, Giuseppe Del Giudice and Armando Carravetta

Department of Civil, Architectural and Environmental Engineering, Università di Napoli Federico II, Via Claudio 21, 80125 Naples, Italy; E-Mails: delgiudi@unina.it (G.D.G.); armando.carravetta@unina.it (A.C.)

* Author to whom correspondence should be addressed; E-Mail: roberta.padulano@unina.it; Tel.: +39-081-768-3462; Fax: +39-081-593-8936.

Abstract: An experimental campaign is undertaken in order to investigate the hydraulic features of a vertical drop shaft, also considering the influence of a venting system consisting of a coaxial vertical pipe, projecting within the drop shaft with different plunging rates. Three different flow regimes are observed: a "weir flow" for very low head values, where the flow profile is subject to the atmospheric pressure; a "full flow" for high head values, where water flows in a pressurized regime along the whole shaft; and a "transitional flow" for intermediate water head values. Weir flow and full flow can be experimentally investigated under steady-state conditions, whereas transitional flow is a pulsating condition, alternately switching from full flow to weir flow. Considering some significant geometric parameters, a head-discharge relation is sought both for the non-vented and for the vented configurations, by means of an energy balance equation, with specific assumptions about intake losses.

Keywords: drop shaft; friction losses; intake losses; pipe Froude number; full flow; weir flow; transitional flow; cavitation

1. Introduction

The evolution of urban texture, along with urban growth, usually leads to the improving and upgrading of existing infrastructures, such as sewer systems. In particular, the increase in the impervious percentage of urban catchment areas implies an increase in surface runoff, which can cause malfunctioning in urban drainage systems, such as basement or street flooding, manhole cover blow-off, up to structural problems.

These disservices can cause huge damages to people or property; therefore, they must be prevented where possible.

The following research was commissioned by the City of Naples in order to solve a problem occurring in one of the drainage basins belonging to its complex combined sewer system. The Via Tasso basin has recently been updated with the construction of a new sewer founded on piles, schematically shown in Figure 1; up to now, that sewer has not been put into operation yet, because the estimated discharge value, which is expected to flow under a return period, T, of 30 years, exceeds the capacity of a hydraulic structure located downstream (which is not shown in the figure). In order to avoid backwater effects, part of the flow must be diverted somewhere before the hydraulic structure, possibly taking advantage of the already existing drainage system to avoid excavation costs; for this purpose, a feasible location was found in the intersection between the new sewer and an existing secondary branch, shown in Figure 1 and placed at the same elevation. At the downstream end of this branch, a vertical drop shaft allows one to overcome an elevation gap; its hydraulic capacity, which is a limiting parameter for the proper functioning of the whole catchment sewer system, is not known.

Under these circumstances, the management works for the catchment imply two different problems, namely concerning the diversion structure and the drop shaft design.

Figure 1. Schematization of the area of interest.
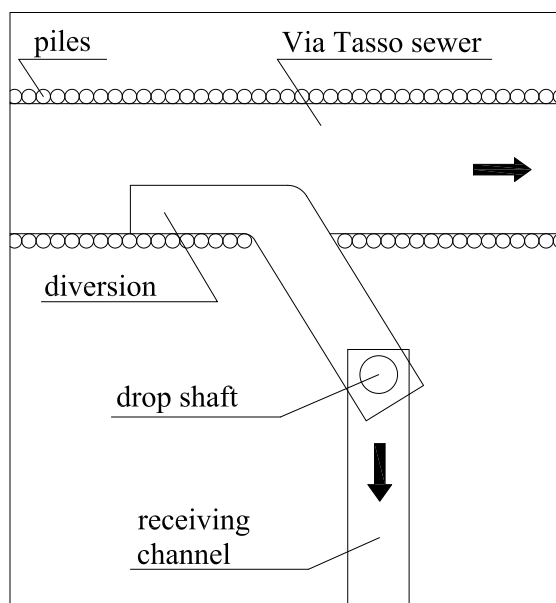

1.1. Diversion Structure

The separation of flow into different parts is typically obtained by using side weirs, which are generally recommended with a subcritical approach flow [1,2]; since the new sewer has a slope of 5%, implying supercritical flow conditions, adopting a side weir might result both in an excessive weir crest length and in the possible occurrence of hydraulic jumps. In particular, the former consequence would entail interacting with the foundation piles, possibly causing an increase in the costs of construction and a danger of structural instability. In addition, the two intersecting pipes are flush, so that a bottom outlet solution cannot be adopted.

In order to overcome these limiting conditions, a frontal rectangular intake diversion structure [3] for supercritical flow was chosen, which consists of a rectangular cross-section channel ("diversion channel") located within the approach flow sewer (Figure 2). Under some simplifying assumptions [3], the device operating conditions are described by the head-discharge relation in Equation (1).

$$q = \dot{b}(1 - \delta) \tag{1}$$

$q = Q_1/Q_0$ is the dimensionless diverted discharge, where Q_1 is the diverted discharge, and Q_0 is the approach flow rate; $b = B_1/B_0$, where B_1 is the diversion structure width and B_0 is the approach flow channel width; $\delta = d/h_0$, where d is the vertical distance of diversion invert from the approach flow sewer bottom and h_0 is the approach flow depth. Equation (1) relates the diversion structure dimensions, namely, width b and the distance from the bottom of the main channel, d, with the discharge value to divert Q_1, so that they can be set accordingly.

Figure 2. Diversion structure views: (**a**) cross-section and (**b**) plan view.
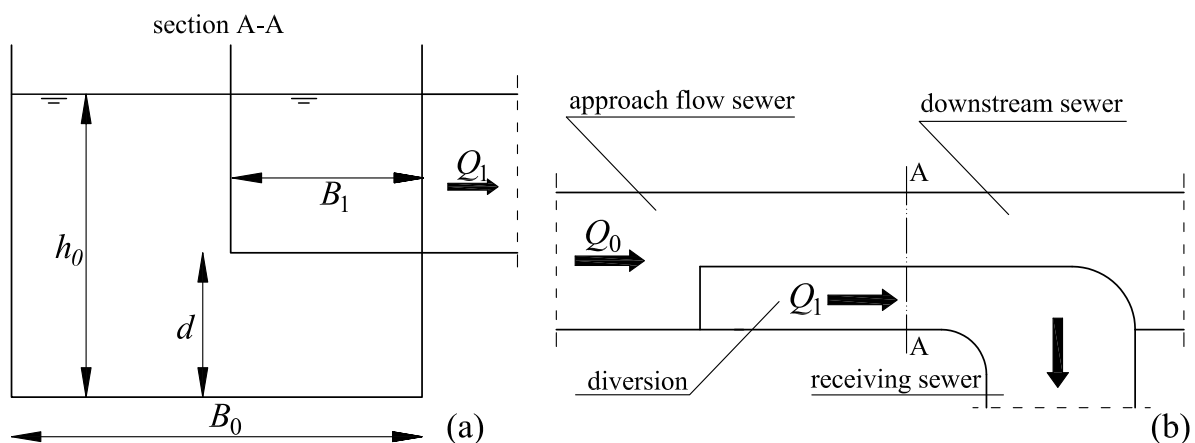
1.2. Drop Shaft

Vertical drop shafts are usually adopted within sewer systems located in hilly regions to convey storm water or sewage across large elevation differences. A drop shaft basically consists of three components, namely, an inlet structure, a vertical pipe and an air venting device. The inlet structure enables a smooth transition from horizontal to vertical flow into the drop shaft; various inlet configurations have been conceived in technical applications and laboratory model studies, such as a vortex, morning glory and square-edged drop shaft [4]. The vertical pipe transports the water to the bottom of the drop shaft, where plunging pools, air cushions or designed hydraulic jumps may be provided as energy dissipators, depending on the difference in elevation.

Since the jet drop is always characterized by a mixture of air and water, air entraining in the vertical barrel should be kept under control, especially in the presence of particularly long vertical pipes. If the air supply is inadequate, the pressure in the drop shaft could fall, so that cavitation may occur at high velocity spots, like the shaft intake or areas where the falling jet impinges onto the shaft walls. Furthermore, even when the shaft is sufficiently supplied with air, there are chances that this air might get compressed and blow back through any available opening in the system, possibly leading to geysering

phenomena [5]. The above-mentioned problems can be avoided by ensuring an adequate air vent system along the drop shaft [6] or immediately before the receiving tunnel [4].

With reference to sewer systems, where the flow rates are highly variable, drop shaft functioning will also vary, depending on whether it works with a free flow (water surface in the receiving channel lies below the shaft base) or with a submerged flow (water surface in the receiving channel lies above the shaft base) [7], and whether the inlet works with a weir flow or with a pipe flow. Generally, a free "weir flow" prevails for small discharges and water heads (h), because air entrainment is ensured as the flow profile undergoes atmospheric pressure over the shaft crest; in this case, discharge is a function of $h^{3/2}$. As the discharge over the crest increases, submergence of the crest begins, and the control section moves from the crest to the inside of the shaft; discharge is then a function of $h^{1/2}$ ("orifice flow"). For a still higher discharge, the condition of "full flow" (or "pipe flow") is reached, and the discharge becomes a linear function of the hydraulic gradient between the pipe inlet and outlet [8–11].

Experimentation is undertaken to determine the relationship between the discharge flowing through the vertical drop shaft and its geometrical characteristics; this will also lead to verifying that the design flow rate can be conveyed to the downward sewer with no significant backwater effects. Besides, a technical solution is provided in order to ensure air venting, in the form of a venting pipe, coaxial to the drop shaft; the influence of its inserting rate into the shaft on the discharged flow is also investigated.

The most significant similar experiments, although not equivalent, were conducted by Binnie [12] and Anwar [13]. Binnie [12] focuses his attention on an overflow pipe, which means a vertical pipe with its intake projected above the tank bottom; a head-discharge relation is qualitatively outlined for increasing heads over the intake. Nevertheless, both the pipe dimensions and the experimented water levels are very small, so that the author himself voices reservations about the applicability of results in higher scaled structures. Anwar [13] is interested in overflow pipes, too, even though some considerations are presented about a flush intake for the vertical pipe; furthermore, a dependence of the discharge on the shape and thickness of pipe edges was found.

2. Experimental Setup and Data Collection

The experimental model consists of a plexiglass rectangular tank with a $0.7 \times 2.07 \times 1.25$ m^3 volume, divided into two equal parts by a filtering wall, namely a detention tank and a filling tank, upstream and downstream of the filter, respectively (Figure 3). The vertical drop shaft, simulated by a plexiglass vertical pipe, with a length of 1 m and an internal diameter of 10 cm, is attached to the bottom center of the filling tank with a square-edged inlet. In order to ensure air venting, a second vertical pipe, with a length of 2 m and an external diameter of 5 cm, can be coaxially housed in the shaft by means of an iron bracket at the tank top and three screws at the plunging end of the venting pipe.

Experiments were performed by varying the discharge value flowing through the system and measuring the water head, which settled in the tank; point gauges were adopted for flow depth measurement with an accuracy of ± 0.5 mm. Both an emptying and a filling path were followed in order to verify whether any hysteretic behavior occurred, with no significant results. Different plunging rates for the venting pipe were also considered, equal to 2-, 4- and 7-times the diameter of the drop shaft, therefore, equal to 20, 40 and 70 cm, respectively (they will be referred to as the 2D, 4D and 7D

conditions). No lower plunging lengths were investigated, in order to avoid a possible interference of the screws with the contraction phenomena occurring at the intake section.

Figure 3. (**a**) Plan view of the experimental setup and (**b**) lateral view of the filling tank.
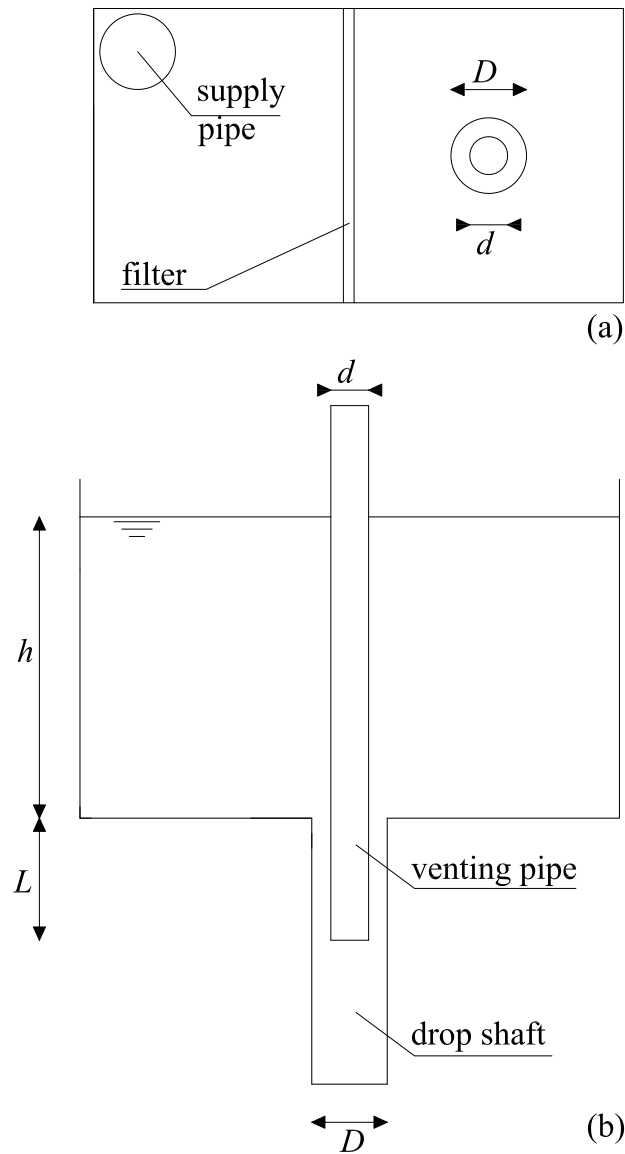
In the following paragraphs, experimental data will be referred to as belonging to three different classes, namely "full flow data", "weir flow data" and "transitional flow data". The first gathers head-discharge data relating to a full flow condition, where the drop shaft volume is entirely occupied by pressurized water; the second gathers data referring to a free surface condition over the intake, where both water and air flow through the vertical pipe, with a central air core. Both types are characterized by an overall stability in water level and pressure values, thus resulting in experimental steady states. Data of the third group relate to a peculiar condition where hydraulic regime alternately switches from full flow to weir flow, the latter with no visible air core; this condition proved very unstable with respect to the water level in the tank, which continuously increased and decreased as the flow was in the weir or full condition, respectively. Consequently, a dynamic measure had to be taken in order to obtain a time plot of h for each discharge value. Table 1 shows a synthesis of the experiments.

Table 1. Experimental data.

ID	h [m]	d [m]	D_{eq} [m]	$D-d$ [m]	L [m]	Q [m³/s]
1	0.033	0.05	0.0866	0.05	0.7	0.00283
2	0.115	0.05	0.0866	0.05	0.7	0.00616
3	0.135	0.05	0.0866	0.05	0.7	0.00963
4	0.175	0.05	0.0866	0.05	0.7	0.01139
5	0.155	0.05	0.0866	0.05	0.7	0.01174
6	0.150	0.05	0.0866	0.05	0.7	0.01347
7	0.170	0.05	0.0866	0.05	0.7	0.01494
8	0.170	0.05	0.0866	0.05	0.7	0.01672
9	0.203	0.05	0.0866	0.05	0.7	0.01737
10	0.290	0.05	0.0866	0.05	0.7	0.01902
11	0.392	0.05	0.0866	0.05	0.7	0.02014
12	0.628	0.05	0.0866	0.05	0.7	0.02218
13	0.872	0.05	0.0866	0.05	0.7	0.02423
14	1.078	0.05	0.0866	0.05	0.7	0.02579
15	0.150	0.05	0.0866	0.05	0.4	0.00714
16	0.170	0.05	0.0866	0.05	0.4	0.01038
17	0.180	0.05	0.0866	0.05	0.4	0.01205
18	0.195	0.05	0.0866	0.05	0.4	0.01372
19	0.185	0.05	0.0866	0.05	0.4	0.01515
20	0.352	0.05	0.0866	0.05	0.4	0.01706
21	0.413	0.05	0.0866	0.05	0.4	0.01791
22	0.648	0.05	0.0866	0.05	0.4	0.02034
23	0.870	0.05	0.0866	0.05	0.4	0.02240
24	1.075	0.05	0.0866	0.05	0.4	0.02419
25	0.090	0.05	0.0866	0.05	0.2	0.00513
26	0.155	0.05	0.0866	0.05	0.2	0.00869
27	0.190	0.05	0.0866	0.05	0.2	0.01099
28	0.195	0.05	0.0866	0.05	0.2	0.01277
29	0.305	0.05	0.0866	0.05	0.2	0.01444
30	0.420	0.05	0.0866	0.05	0.2	0.01604
31	0.620	0.05	0.0866	0.05	0.2	0.01842
32	0.841	0.05	0.0866	0.05	0.2	0.02076
33	1.078	0.05	0.0866	0.05	0.2	0.02244
34	0.048	0	0.1	0.10	1	0.00274
35	0.038	0	0.1	0.10	1	0.00357
36	0.123	0	0.1	0.10	1	0.00645
37	0.080	0	0.1	0.10	1	0.00706
38	0.120	0	0.1	0.10	1	0.01219
39	0.160	0	0.1	0.10	1	0.01625
40	0.200	0	0.1	0.10	1	0.02016
41	0.195	0	0.1	0.10	1	0.02395
42	0.230	0	0.1	0.10	1	0.02534
43	0.145	0	0.1	0.10	1	0.02738
44	0.160	0	0.1	0.10	1	0.02886
45	0.308	0	0.1	0.10	1	0.03398
46	0.540	0	0.1	0.10	1	0.03688
47	0.820	0	0.1	0.10	1	0.04010
48	1.060	0	0.1	0.10	1	0.04274

3. Results

The collected data were assembled in a head-discharge graph, as shown in Figure 4; four curves can be recognized, which correspond, from right to left, to the non-vented, 7D, 4D and 2D conditions. The plunged lengths were also observed to be the physical regions where full flow occurs, whereas a mixture of air and water was seen beyond the terminal section of the coaxial pipe. In accordance with the state-of-the-art, for all the curves, full flow data are approximately linearly distributed in the upper right part, so that a small variation in the discharge value causes a great change in the water level. On the opposite, non-full flow data (namely, weir flow and transitional flow data) distribute in the lower left part, with a totally different curvature, such that a great variation in the discharge value causes a small change in the water level. As regards transitional flow, the average water head was related to the imposed discharge to obtain the square marks in Figure 4.

As was expected, the non-vented condition is characterized by the greatest carrying capacity, meaning that, for a fixed water head over the shaft intake, the greatest discharge value flows through the device among all the investigated configurations, because of the larger effective cross-section. As regards the vented conditions, they are characterized by the same cross-section value, since the same diameter was used for the coaxial pipe, but the capacity was found to increase with the plunging rate, as can be seen in Figure 4.

Figure 4. (**a**) Experimental data and (**b**) focus on full flow data.
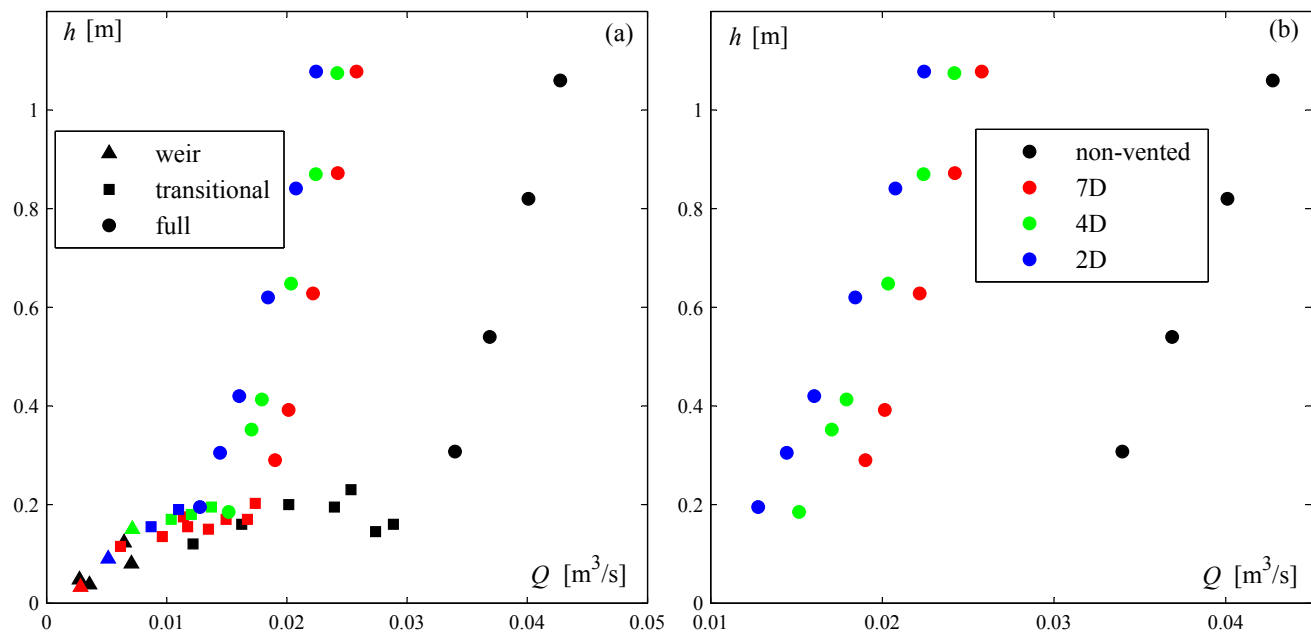
4. Discussion

4.1. Non-Vented Configuration

At first, attention was focused on the easiest among the investigated configurations, that is, the one without any coaxial pipe. The Bernoulli theorem between points A and B of a trajectory, with A

belonging to the free surface of the filling tank and B belonging to the terminal cross-section of the vertical pipe, was applied, assuming the velocity head, $v_A^2/2g$, to be negligible and the relative pressure heads, P_A/γ and P_B/γ, to be null. These considerations lead to the following head-discharge equation for the non-vented configuration:

$$h + L = \frac{v_B^2}{2g} + \frac{f}{4R} \cdot \frac{v_B^2}{2g} \cdot [L - 8 \cdot R] + \xi \cdot \frac{v_B^2}{2g} = (1 + \beta + \xi) \cdot \frac{v_B^2}{2g} \tag{2}$$

which leads to the following head-discharge equation for the non-vented configuration:

$$Q = \frac{\pi D^2}{4} \cdot \sqrt{\frac{1}{1 + \beta + \xi}} \cdot \sqrt{2g \cdot (h + L)} \tag{3}$$

with $\beta = f \cdot [L - 8 \cdot R]/4R$. Q is the discharge flowing in the pipe, in [m^3 s^{-1}], with a head, h, in [m], over the inlet; R is the hydraulic radius, in [m]; L is the length of the vertical pipe, in [m], whereas $8R = 2D$ is the pipe portion, which is the nearest to the shaft inlet, where flow trajectories cannot be considered straight and parallel; $\pi D^2/4$ is the hydraulic section. Friction losses, expressed by the Darcy-Weisbach equation, take place along the length, $L - 8R$; the smooth pipe theory was adopted to compute the friction factor, f, in accordance with the experimented Reynolds numbers, ranging between about 4×10^5 and 5×10^5, and with the typical roughness values for pipes in plastic materials ranging between 0.0015 and 0.0070 [2]. As regards minor losses, a local loss coefficient, ξ, was considered by analogy with the square-edged entrance model [14]. The particular choice of $8R$ for the minor losses extent was made by observing the pressure distribution along the shaft; as shown in Figure 5, the pressure distribution is almost perfectly linear from that section on.

Figure 5. Pressure distribution along the drop shaft wall (experiment 48).
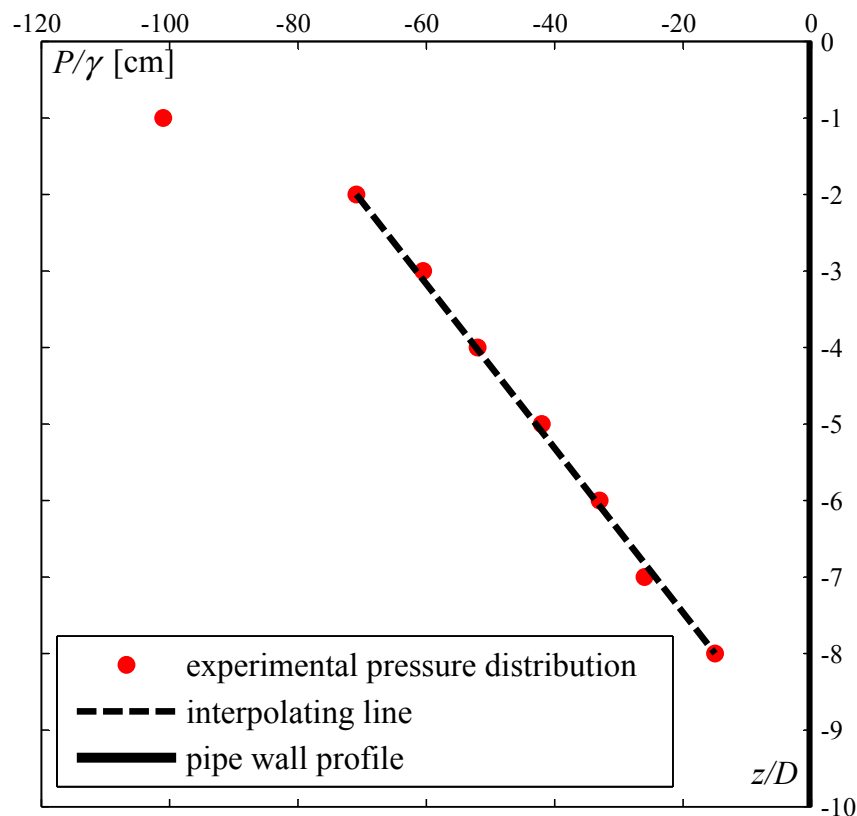
Considering $\xi = 0.5$ [14] provided a poor adaptation of Equation (3) to experimental data; therefore, a calibration procedure was applied to find out the ξ value that best fitted the data. At first, ξ was considered as being variable with the water level, h; however, as Figure 6 shows, it can be considered fixed. Calibration proved to be highly satisfactory with a constant value equal to 0.27.

Figure 6. Local loss parameter, ξ, *vs.* water head, h.
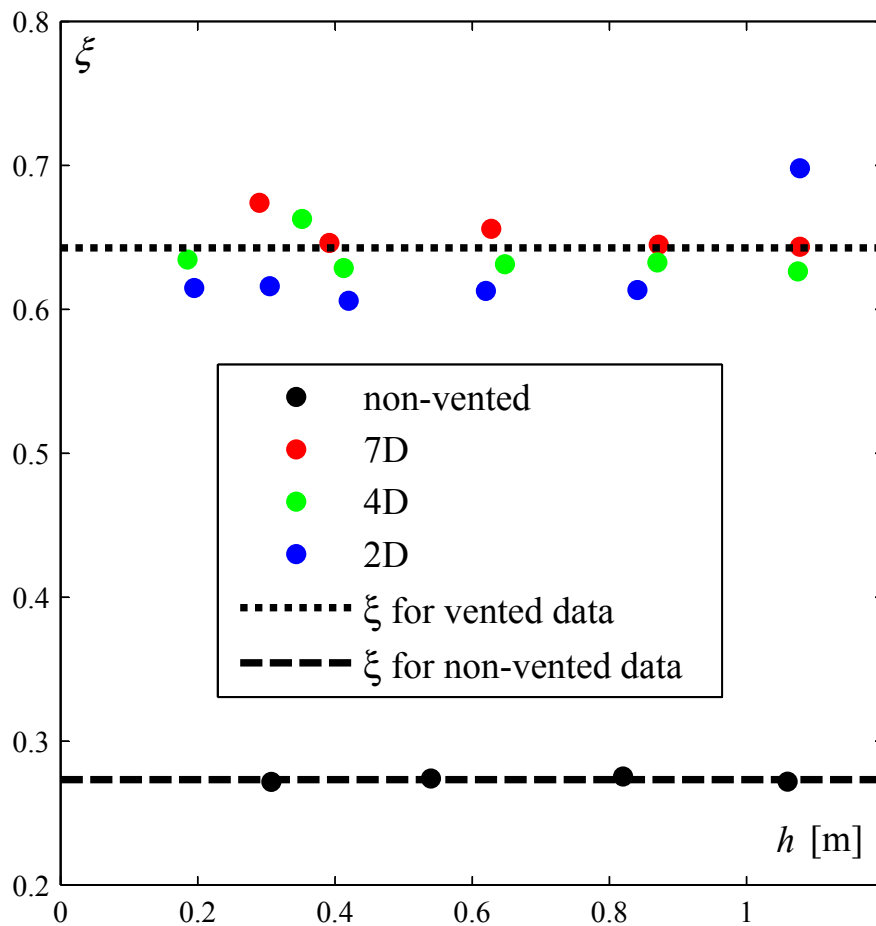
4.2. Vented Configurations

Equations (2) and (3) can be applied to the vented configurations, noticing that for the annular section, the hydraulic radius R is equal to $(D - d)/4$, and the hydraulic section is equal to $\pi D_{eq}^2/4$, where $D_{eq}^2 = \sqrt{D^2 - d^2}$, D being the inner shaft diameter and d the outer coaxial pipe diameter. Furthermore, as full flow is observed up to the final cross-section of the coaxial pipe, point B of the Bernoulli theorem is located in this section.

The same considerations can be held for friction losses, which can be expressed by a parameter, $\beta(Re)$, and for minor losses, whose representative parameter, ξ, can be considered fixed. The calibration procedure provides $\xi = 0.64$ (as shown in Figure 6); this is consistent with the consideration that local intake losses allegedly are a function of the inlet shape, so that a different value is expected in the two cases. The results of calibration corroborate the assumptions concerning the constant loss parameter. Table 2 provides significant parameters for full flow data.

Table 2. Experimental full flow data.

id	$Q[\mathrm{m^3/s}]$	$h[\mathrm{m}]$	$v[\mathrm{m/s}]$	Re	f	ξ	β	$Q_\mathrm{e}[\mathrm{m^3/s}]$
10	0.01902	0.290	3.23	161,440	0.0158	0.674	0.189	0.01957
11	0.02014	0.392	3.42	170,959	0.0155	0.646	0.186	0.02056
12	0.02218	0.628	3.77	188,256	0.0152	0.656	0.182	0.02267
13	0.02423	0.872	4.11	205,660	0.0148	0.645	0.178	0.02466
14	0.02579	1.078	4.38	218,948	0.0146	0.644	0.175	0.02623
19	0.01515	0.185	2.57	128,610	0.0167	0.635	0.100	0.01504
20	0.01706	0.352	2.90	144,768	0.0162	0.663	0.097	0.01706
21	0.01791	0.413	3.04	152,054	0.0160	0.629	0.096	0.01774
22	0.02034	0.648	3.45	172,660	0.0155	0.631	0.093	0.02014
23	0.02240	0.870	3.80	190,125	0.0151	0.633	0.091	0.02217
24	0.02419	1.075	4.11	205,363	0.0148	0.626	0.089	0.02389
28	0.01277	0.195	2.17	108,372	0.0174	0.615	0.035	0.01236
29	0.01444	0.305	2.45	122,528	0.0169	0.616	0.034	0.01398
30	0.01604	0.420	2.72	136,124	0.0165	0.606	0.033	0.01549
31	0.01842	0.620	3.13	156,389	0.0159	0.613	0.032	0.01781
32	0.02076	0.841	3.52	176,220	0.0154	0.613	0.031	0.02007
33	0.02244	1.078	3.81	190,445	0.0151	0.698	0.030	0.02224
46	0.03688	0.540	4.70	469,541	0.0121	0.274	0.097	0.03691
47	0.04010	0.820	5.11	510,564	0.0118	0.275	0.095	0.04012
48	0.04274	1.060	5.44	544,167	0.0116	0.272	0.093	0.04269

Note: Q_e is the estimated discharge, computed by means of Equation (3), with fixed values for ξ.

4.3. Adimensionalization of Results

In accordance with [15], a dimensionless expression of results is provided for pressurized flow, once the following dimensionless parameters are defined: the pipe Froude number, $F_D = Q/\sqrt{gD_{eq}^5}$, the dimensionless water head, $Y = h/D_{eq}$, the dimensionless pipe length, $\lambda = L/D_{eq}$, and $\theta = D_{eq}/(D-d)$. Dividing the terms in Equation (3) for $\sqrt{gD_{eq}^5}$, the following relation is obtained:

$$\frac{Q}{\sqrt{gD_{eq}^5}} = \frac{\pi\sqrt{2}}{4} \cdot \sqrt{\frac{1}{1 + \beta + \xi}} \cdot \sqrt{\frac{h}{D_{eq}} + \frac{L}{D_{eq}}} \tag{4}$$
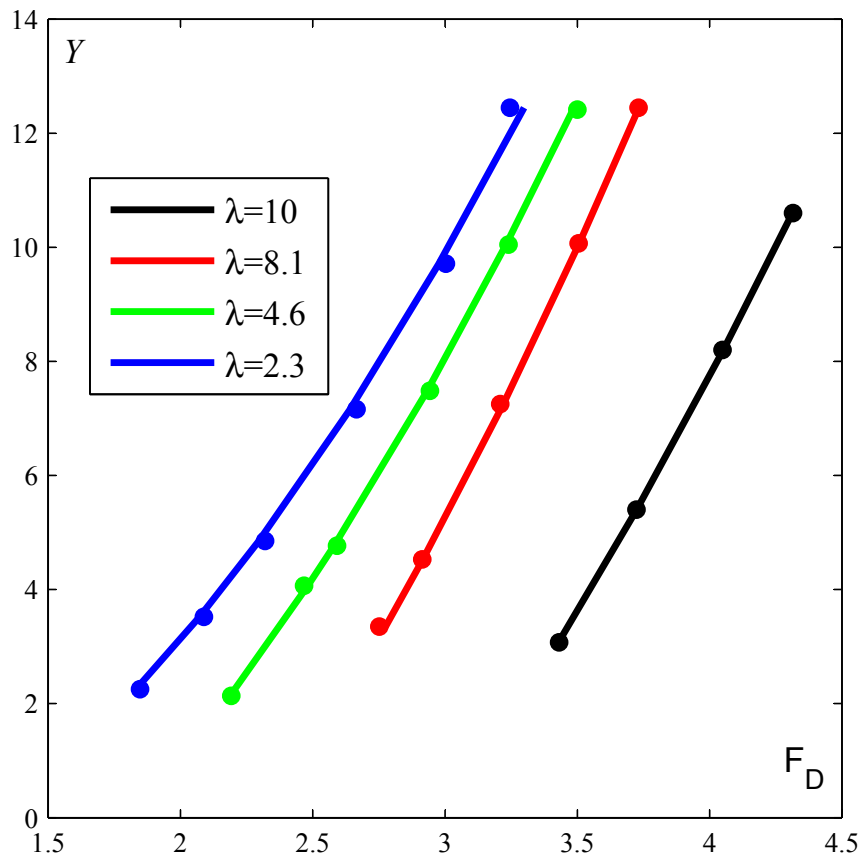
which specifies the non-vented configuration in the following equation :

$$F_D = 1.11 \cdot \left[\frac{Y + \lambda}{1.27 + f \cdot (\lambda - 2)} \right]^{0.5} \tag{5}$$

and in the following equation, the vented configurations:

$$F_D = 1.11 \cdot \left[\frac{Y + \lambda}{1.64 + f \cdot (\lambda\theta - 2)} \right]^{0.5} \tag{6}$$

with all the other symbols previously defined. Figure 7 shows the results of adimensionalization.

Figure 7. Dimensionless results [Equations (5) and (6)].

5. Conclusions

An experimental campaign was undertaken in order to investigate the working conditions of a vertical drop shaft, with and without a venting system, made up of a coaxial vertical pipe with variable plunging rates.

Results of the experiments show that the system can experience three different working conditions. The first ("weir flow") occurs for water heads lower than about the shaft diameter and is characterized by stable values of water levels; the drop shaft is occupied by an air-water mixture with a central air core, so that the entering flow profile undergoes atmospheric pressure. The second ("full flow") regime occurs for head values higher than about two-times the diameter of the shaft and, as the weir flow, is a steady-state; in this case, the shaft is entirely occupied by water flowing in a pressurized regime. The third ("transitional flow") regime occurs for water heads ranging between one and two times the diameter of the shaft; it is a very unstable and pulsating condition with significant recurring variations in water head and discharge values. The shaft is alternately occupied by pressurized water and an air-water mixture; however, in the latter case, no air core is visible, since the central vortex is gulped.

As regards the head-discharge relation, full flow shows a rapid increase in the water heads for minimum flow rate variations, whereas both weir and transitional flow (the latter with respect to the average water heads) are characterized by an opposite behavior, with slow changes in the water heads for significant variations of discharge.

Experiments showed that the unvented drop shaft has the greatest carrying capacity, which rapidly falls when the coaxial pipe is inserted, namely because of a huge reduction in the hydraulic section. Furthermore, capacity decreases with decreasing venting pipe plunging rate; indeed, the lowest capacity was experienced for the 2D configuration. However, the lower head values in the vented cases cause a significant reduction, also, in the depression values along the shaft, so avoiding the possible danger of cavitation.

The interpretation of the results mainly focused on full flow data, since the pulsating behavior of non-full data would need more detailed measures for both discharge and water level values. A correlation was sought between water head and discharge by applying a physical law, namely, the Bernoulli theorem, where friction and minor losses were expressed by means of parameters β and ξ, respectively, where β depends on the specific resistance law adopted. An appropriate analysis of experimental data showed that it was possible to assume ξ as a constant with respect to the water head, h, being a function of the inlet shape alone. The literature value, $\xi = 0.5$, proved unsatisfactory, whereas experimental data provided $\xi = 0.27$ for the non-vented case and $\xi = 0.64$ for the vented configurations.

Acknowledgements

Conflicts of Interest

The authors declare no conflict of interest.

References

1. Del Giudice, G.; Hager, W.H. Sewer side weir with throttling pipe. *J. Irrig. Drain. Eng.* **1999**, *125*, 298–306.
2. Hager, W. *Wastewater Hydraulics: Theory and Practice*, 2nd ed.; Springer: Berlin, Germany, 2010.
3. Del Giudice, G.; Padulano, R.; Carravetta, A. Novel diversion structure for supercritical flow. *J. Hydraul. Eng.* **2013**, *139*, 84–87.
4. Williams, O. *Tunnels and Shafts in Rock*; Manual No. 1110-2-2901; U.S. Army Corps of Engineers: Washington, DC, USA, 1997.
5. Rajaratnam, N.; Mainali, A.; Hsung, C.Y. Observations on flow in vertical dropshafts in urban drainage systems. *J. Environ. Eng.* **1997**, *5*, 486–491.
6. Guo, Q.; Song, C.C.S. *Hydraulic Transient Analysis of TARP Phase II O'Hare System*; Project Report 276; St. Anthony Falls Hydraulic Laboratory: Minneapolis, MN, USA, 1988.
7. Viparelli, M. Air and water currents in vertical shafts. *La Huille Blanche* **1961**, *16*, 857–869.
8. United States Bureau of Reclamation (USBR). *Design of Small Dams*; USBR: Washington, DC, USA, 1987.
9. Fattor, C.A.; Bacchiega, J.D. Analysis of instabilities in the change of regime in morning-glory spillways. *Proc. Congr. Int. Assoc. Hydraul. Res.* **2001**, *29*, 656–662.
10. Khatsuria, R.M. *Hydraulics of Spillways and Energy Dissipators*; Civil and Environmental Engineering Series, Marcel Dekker: New York, NY, USA, 2005.

11. Robinson, A.; Morvan, H.; Eastwick, C. Computational investigations into draining in an axisymmetric Vessel. *J. Fluid. Eng.* **2010**, *132*, doi:10.1115/1.4003151.

12. Binnie, A. The use of a vertical pipe as an overflow for a large tank. In *Proceedings of the Royal Society of London. Series A. Mathematical and Physical Sciences*; The Royal Society: London, UK, 1938; pp. 219–237.

13. Anwar, H.O. Coefficients of discharge for gravity flow into vertical pipes. *J. Hydraul. Res.* **1965**, *3*, 1–19.

14. Potter, M.C.; Wiggert, D.C.; Ramadan, B.H. *Mechanics of Fluids*, 4th ed.; Cengage Learining: Hampshire, UK, 2011.

15. Hager, W.H.; del Giudice, G. Generalized culvert design diagram. *J. Irrig. Drain. Eng.* **1998**, *124*, 271–274.